nature cell biology

ARTICLES

The endoplasmic reticulum is the site of cholesterol-induced cytotoxicity in macrophages

Bo Feng[1], Pin Mei Yao[1], Yankun Li[1], Cecilia M. Devlin[1], Dajun Zhang[1], Heather P. Harding[2], Michele Sweeney[3], James X. Rong[4], George Kuriakose[1], Edward A. Fisher[4], Andrew R. Marks[3], David Ron[2] and Ira Tabas[1,5]

Excess cellular cholesterol induces apoptosis in macrophages, an event likely to promote progression of atherosclerosis. The cellular mechanism of cholesterol-induced apoptosis is unknown but had previously been thought to involve the plasma membrane. Here we report that the unfolded protein response (UPR) in the endoplasmic reticulum is activated in cholesterol-loaded macrophages, resulting in expression of the cell death effector CHOP. Cholesterol loading depletes endoplasmic reticulum calcium stores, an event known to induce the UPR. Furthermore, endoplasmic reticulum calcium depletion, the UPR, caspase-3 activation and apoptosis are markedly inhibited by selective inhibition of cholesterol trafficking to the endoplasmic reticulum, and *Chop*$^{-/-}$ macrophages are protected from cholesterol-induced apoptosis. We propose that cholesterol trafficking to endoplasmic reticulum membranes, resulting in activation of the CHOP arm of the UPR, is the key signalling step in cholesterol-induced apoptosis in macrophages.

Macrophages accumulate free cholesterol in advanced atherosclerotic lesions, resulting in macrophage apoptosis and progression of lesions[1–8]. Previous studies with cultured macrophages have elucidated downstream apoptotic events induced by free cholesterol loading[8–11]. However, the proximal free-cholesterol-induced events that trigger apoptosis have not yet been identified. It was shown recently that free-cholesterol-induced macrophage death could be blocked by micromolar concentrations of certain amphipathic amines that are known to interfere with cholesterol trafficking from late endosomes to other cellular sites, particularly the plasma membrane[9,12]. On the basis of these observations and previous *in vitro* data showing that plasma membrane proteins function poorly in free-cholesterol-enriched membranes[13], it was proposed that death of free-cholesterol-loaded macrophages was triggered by abnormal enrichment of the plasma membrane with free cholesterol[12].

Cholesterol derived from endocytosed lipoproteins is also trafficked from late endosomes to other cellular sites, such as the endoplasmic reticulum. Because the cholesterol content of endoplasmic reticulum membranes is particularly low[14], the function of this organelle is likely to be particularly sensitive to abnormal enrichment with free cholesterol. Perturbations of endoplasmic reticulum function from many causes activate a signalling pathway referred to as the UPR[15], resulting in transcriptional activation of genes whose products promote the capacity of the endoplasmic reticulum to process client proteins, synthesize phospholipids and re-esterify sterols[16]. These last two responses may be involved in reducing the burden of free cholesterol accumulation in the endoplasmic reticulum and other cell membranes[17]. However, the UPR also activates signalling pathways that promote programmed cell death, including activation of a specific caspase[18], Jun *N*-terminal stress-activated protein kinases[19,20], and the transcription factor CHOP[21,22]. These observations suggested that free cholesterol loading of endoplasmic reticulum membranes might contribute to macrophage apoptosis.

In this study we used genetic and pharmacological tools that selectively perturb cholesterol trafficking from late endosomes to specific cellular sites, allowing us to explore further the basis of free-cholesterol-induced apoptosis in macrophages. Our findings implicate endoplasmic-reticulum-based signals in the death of free-cholesterol-loaded macrophages and thus provide new insight into the relationship between cholesterol homeostasis in the endoplasmic reticulum membrane and endoplasmic reticulum function. Moreover, the data suggest a novel cellular mechanism for cholesterol-induced macrophage death in advanced atherosclerotic lesions.

RESULTS

The plasma membrane is not the site of cholesterol-induced apoptosis

In macrophages that have ingested lipoprotein particles, micromolar concentrations of the amphipathic amine U18666A inhibit multiple pathways of cholesterol trafficking from late endosomes[23]. However, when used at nanomolar concentrations, U18666A selectively interferes with cholesterol trafficking to the endoplasmic reticulum without substantively affecting the transfer of cholesterol to the

[1]Departments of Medicine and Cell Biology, Columbia University, New York, NY 10032, USA. [2]Skirball Institute, New York University School of Medicine, New York, NY 10016, USA. [3]Department of Physiology and Cellular Biophysics, Center for Molecular Cardiology, Columbia University, New York, NY 10032, USA. [4]Department of Medicine and The Zena and Michael A. Wiener Cardiovascular Institute, Mount Sinai School of Medicine, New York, NY 10029, USA.
[5]Correspondence should be addressed to I.T. (e-mail: iat1@columbia.edu).

Published online: 10 August 2003; DOI: 10.1038/ncb1035

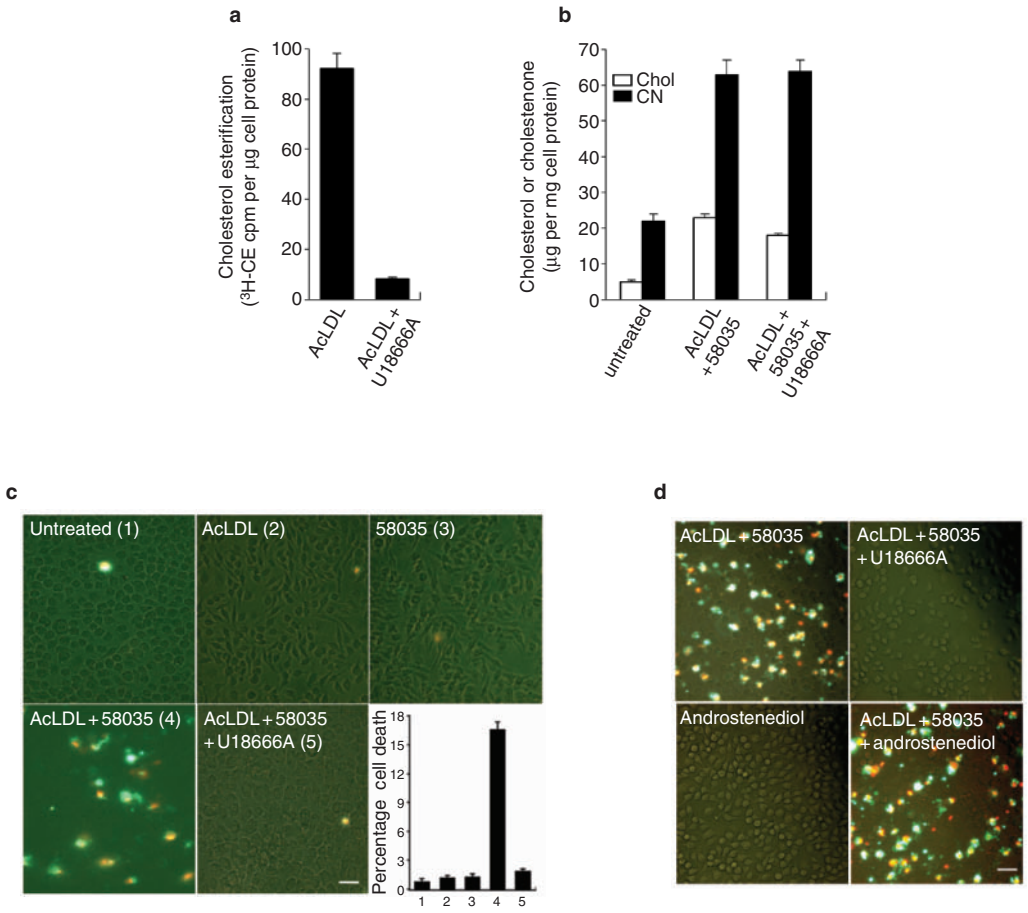

Figure 1 Free-cholesterol-induced apoptosis in macrophages is blocked by a low dose of U18666A. (**a**) Esterification of ^{3}H-cholesterol (a measure of cholesterol trafficking to endoplasmic reticulum membranes) in cultured mouse peritoneal macrophages incubated for 5 h with medium containing 50 μg ml^{-1} ^{3}H-cholesterol-labelled acetyl-LDL in the absence or presence of 70 nM U18666A. Results are the mean ± s.e.m. ($n = 3$) of ^{3}H-cholesteryl ester formed (in cpm per μg cell protein). (**b**) Accessibility of cellular cholesterol to cholesterol oxidase (a measure of plasma membrane cholesterol) in fixed macrophages after incubation for 4 h with medium alone or medium containing 50 μg ml^{-1} acetyl-LDL in the absence or presence of 10 μg ml^{-1} 58035 or 70 nM U18666A. The mass (in μg per mg cell protein) of cholesterol (Chol, open bars), which is the cholesterol-oxidase-inaccessible pool of intracellular cholesterol, and of cholestenone (CN, solid bars), which is the cholesterol-oxidase-accessible pool of plasma membrane cholesterol are shown. (**c**) Alexa-488–annexin V staining (green) and PI staining (red-orange) to assess death of macrophages incubated for 8 h under the same conditions as in **a**, with the inclusion of two additional controls, acetyl-LDL alone and 58035 alone. Representative fluorescence images and quantitative cell death data from five fields of cells for each condition are shown, expressed as the percentage of total cells that stained with annexin V or PI (mean ± s.e.m.; $n = 5$ fields of cells, where each field contained approximately 200 cells). Numbers under each bar refer to the five conditions depicted in the images. Scale bar represents 10 μm for each of the five images. (**d**) Alexa-488–annexin V and PI staining of macrophages incubated for 16 h under the indicated conditions. Scale bar represents 10 μm for each of the four images.

plasma membrane[23]. Here, we confirm these observations in mouse peritoneal macrophages by showing that treatment with nanomolar concentrations of U18666A reduced re-esterification of ingested cholesterol (an event that occurs in the endoplasmic reticulum) by 90% (Fig. 1a), but had no effect on accumulation of cholesterol in the plasma membrane. Effects at the plasma membrane were assayed by analysing accessibility of plasma membrane cholesterol to exogenous cholesterol oxidase in lipoprotein-loaded, gluteraldehyde-fixed cells (Fig. 1b) and by extractability of cholesterol by methyl-β-CD at 4 °C (data not shown). U18666A alone has no direct inhibitory effect on the acyl-CoA:cholesterol acyltransferase (ACAT) enzyme[23]. Thus, low-dose U18666A provides a useful tool to selectively examine the role of cholesterol trafficking to the endoplasmic reticulum in macrophage apoptosis.

High concentrations of U18666A that completely inhibit cholesterol trafficking were previously shown to block macrophage death induced by cholesterol loading[12]. Therefore, we tested whether a low dose of U18666A, which selectively impair trafficking to the endoplasmic reticulum membrane, also protect macrophages from apoptosis. Free cholesterol accumulation (loading) was effected by incubating macrophages with acetyl-low-density lipoprotein (acetyl-LDL) in the presence of the ACAT inhibitor 58035, which inhibits cholesterol re-esterification and thus prevents the conversion of the ingested cholesterol into cholesteryl ester[8,24]. Free cholesterol loading was toxic to macrophages, resulting in apoptosis (Fig. 1c), as predicted from previous analysis with TUNEL and caspase assays[10]. However, even at a low dose that selectively impairs cholesterol trafficking to the endoplasmic reticulum, U18666A treatment protected macrophages from free-cholesterol-induced apoptosis (Fig. 1c).

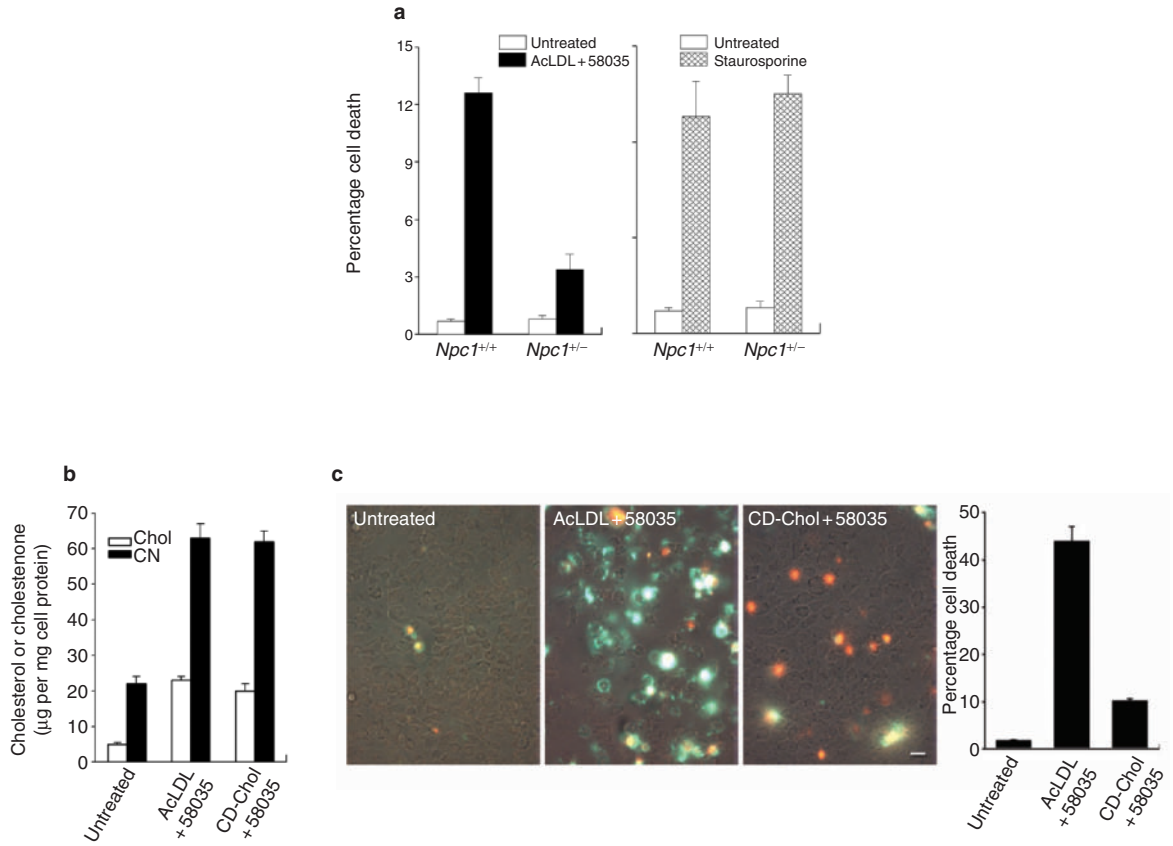

Figure 2 The endoplasmic reticulum, not the plasma membrane, is the site of cholesterol-Induced apoptosis. (**a**) Quantification of annexin V and PI staining of macrophages from wild-type or *Npc1*$^{+/-}$ mice incubated for 8.5 h with medium alone, medium containing 50 μg ml^{-1} acetyl-LDL and 10 μg ml^{-1} 58035, or medium containing 50 nM staurosporine. The percentage of total cells stained with annexin V or PI (mean ± s.e.m.; $n = 5$ fields of cells, where each field contained approximately 200 cells) are shown. (**b**) Alteration in the mass of the cholesterol-oxidase-accessible pool of plasma membrane cholesterol after a 4-h incubation of macrophages with medium alone, medium containing 25 μg ml^{-1} acetyl-LDL and 10 μM 58035, or medium containing 5 mM methyl-β-cyclodextrin:cholesterol (5:1 mass ratio) and 10 μM 58035 (CD-Chol). Data are displayed as in Fig. 1b. (**c**) Alexa-488–annexin V and PI staining of macrophages incubated for 8.5 h in the absence or presence of CD-cholesterol, using the medium described in **b**. Representative fluorescence images (left) and quantitative data (right) are shown (mean ± s.e.m.; $n = 5$ fields of cells, where each field contained approximately 200 cells). Scale bar represents 10 μm.

U18666A treatment failed to protect macrophages from apoptosis induced by the phosphatase inhibitor, staurosporine, attesting to the specificity of its protective effect (data not shown). Moreover, androstenediol, a structurally related homologue of U18666A that does not block cholesterol trafficking to the endoplasmic reticulum in mouse peritoneal macrophages[25], did not block free-cholesterol-induced cell death, even at concentrations greater than 1 μM (Fig. 1d).

NPC1 is important for the intracellular trafficking of cholesterol[26]. Previously, we noted that peritoneal macrophages derived from *Npc1*$^{+/-}$ mice have a cholesterol trafficking defect that closely mimics that of cells treated with low-dose U18666A[27]. Therefore, we compared free-cholesterol-induced death in macrophages from *Npc1*$^{+/+}$ and *Npc1*$^{+/-}$ mice. Similarly to macrophages treated with a low dose of U18666A, *Npc1*$^{+/-}$ macrophages were markedly protected from free-cholesterol-induced death, but not from other inducers of macrophage apoptosis (Fig. 2a).

These data are consistent with a role for cholesterol trafficking to the endoplasmic reticulum, rather than to the plasma membrane, in free-cholesterol-induced apoptosis. To test this model further, we directly loaded the plasma membrane of macrophages with excess free cholesterol by incubating cells with cholesterol-saturated cyclodextrin (CD, a cyclic oligosaccharide that solubilizes free cholesterol) in the presence of 58035. CD-cholesterol, which bypasses the endocytic route used by lipoproteins, transfers free cholesterol directly to the plasma membrane but inefficiently to the endoplasmic reticulum[28–30]. CD-cholesterol increased plasma membrane free cholesterol levels to that found in macrophages incubated with acetyl-LDL and 58035 (Fig. 2b). However, cell death was significantly reduced in cells incubated with CD-cholesterol, compared with cells loaded through the endocytic lipoprotein pathway (Fig. 2c). These data suggest that the accumulation of excess free cholesterol in the plasma membrane is not sufficient to induce apoptosis in free-cholesterol-loaded macrophages, further highlighting the importance of the endoplasmic reticulum in this process.

Cholesterol loading of macrophages activates the UPR

As shown above, the protective effects of low-dose U18666A and the *Npc1*$^{+/-}$ mutation are associated with inhibition of cholesterol trafficking to the endoplasmic reticulum. Because endoplasmic reticulum membranes normally contain low levels of cholesterol[14], we sought to determine if excess trafficking of free cholesterol to the endoplasmic reticulum would perturb organelle function. To this end, we monitored UPR activity in free-cholesterol-loaded macrophages under conditions that were permissive or non-permissive for cholesterol trafficking to

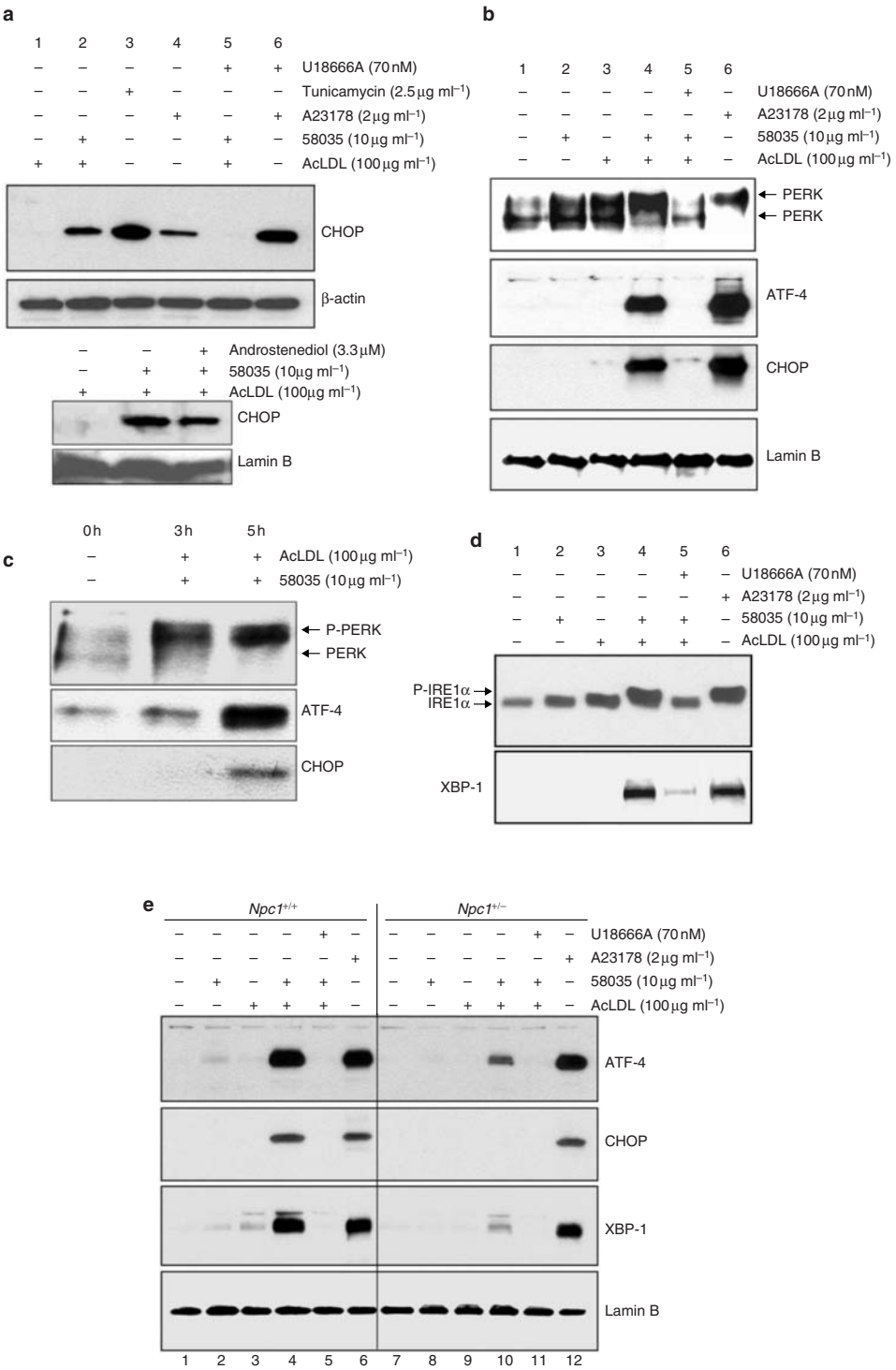

Figure 3 Free cholesterol loading of macrophages activates the UPR. (**a**) CHOP and β-actin immunoblots of whole-cell macrophage extracts incubated under control or free cholesterol loading conditions. Macrophages were incubated for 5 h in medium containing reagents and acetyl-LDL alone or acetyl-LDL and 58035 before immunoblotting for CHOP. Lamin B was used as a loading control. (**b**, **c**) PERK, ATF-4, CHOP and lamin B immunoblots of nuclei-free or nuclear extracts of macrophages incubated under control or free cholesterol loading conditions. In **b**, macrophages were treated for 5 h in medium containing reagents, as indicated. For detection of PERK, nuclei-free cell extracts were immunoprecipitated with anti-PERK antiserum and then immunoblotted. For detection of ATF-4 and CHOP, immunoblots were performed on nuclear extracts. Lamin B was used as a loading control. In **c**, macrophages were either extracted before the incubation period or incubated for 3 or 5 h with medium containing reagents, as indicated. Samples were then immunoblotted for PERK, ATF-4 and CHOP, as in **b**. (**d**) IRE1α and XBP-1 immunoblots of nuclei-free or nuclear extracts, respectively, of macrophages incubated under the same control or free cholesterol loading conditions as in **b**. (**e**) ATF-4, CHOP, XBP-1 and lamin B immunoblots of macrophages from *Npc1*$^{+/+}$ or *Npc1*$^{+/-}$ mice incubated under the same conditions as in **b** and **d**.

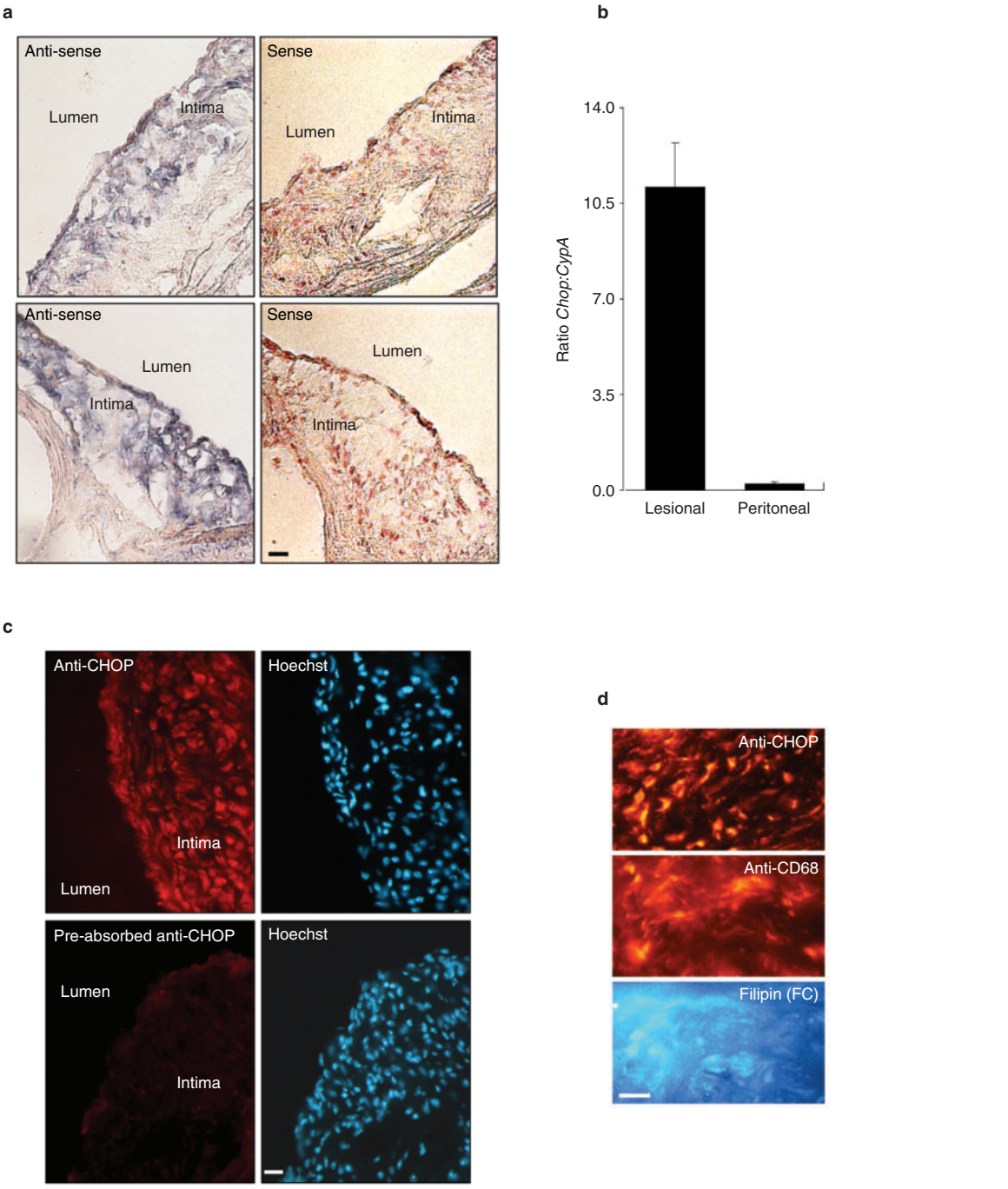

Figure 4 CHOP is expressed in the atherosclerotic lesions of *Apoe*$^{-/-}$ mice. (**a**) *Chop in-situ* histohybridization of proximal aortic atherosclerotic lesion sections from *Apoe*$^{-/-}$ mice fed the Western-type diet for 13 weeks. Representative images using the anti-sense *Chop* probe (dark blue) are shown in the two left panels, whereas adjacent sections stained with the control, sense probe, are shown in the two right panels. Sections were counter-stained with Fast Red (reddish brown) to show the nuclei of the lesional cells. Scale bar represents 20 μm for each of the four images. (**b**) Quantitative *Chop* RT–PCR of RNA from lesional macrophages (using laser capture microdissection) and from resident peritoneal macrophages (using mice similar to those shown in **a**). Results are the mean ± s.e.m. ($n = 3$ Taqman repeats of the RNA samples) of the *Chop*:*CypA* (standard) ratio. (**c**) Anti-CHOP and Hoechst-33258 (nuclear) double-immunofluorescence microscopy analysis, showing sections of a proximal aortic lesion from a mouse similar to that shown in **a**. The top left and right panels show a representative section of the CHOP (red) and nuclear (blue) signals, respectively. The bottom left panel shows the CHOP signal after absorption of the antibody with its cognate peptide. The bottom right panel shows nuclear staining of this section. Scale bar represents 10 μm for each of the four images. (**d**) Anti-CHOP, anti-CD68 (macrophages) and filipin (free cholesterol) staining of three sections of a proximal aortic lesion from a mouse similar to that shown in **a**. Scale bar represents 10 μm for each of the four images.

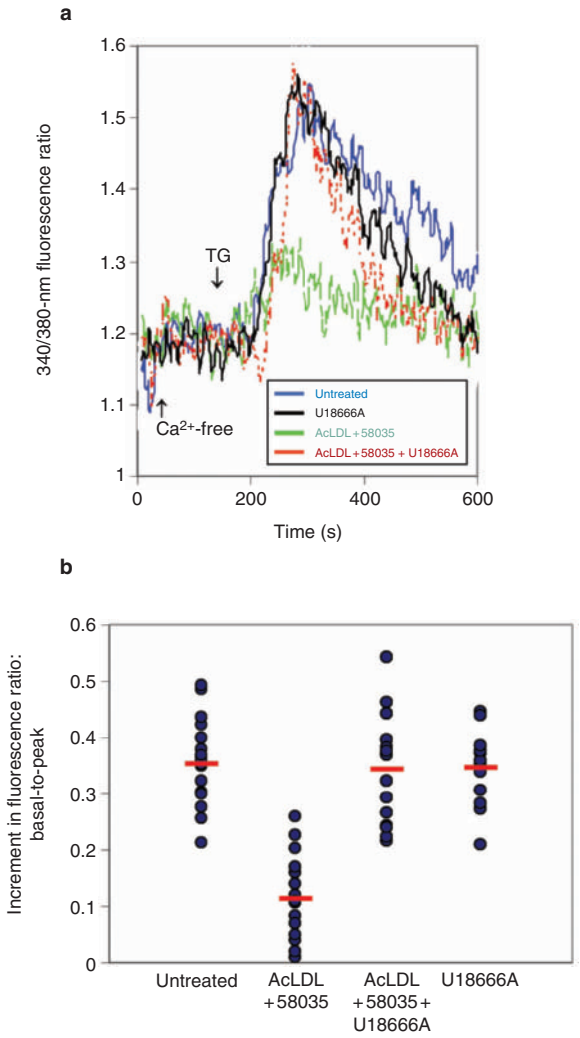

Figure 5 Free cholesterol loading depletes endoplasmic reticulum calcium stores. (**a**) Assessment of endoplasmic reticulum calcium stores in macrophages incubated for 2.5 h with medium alone (untreated); 70 nM U18666A; 100 μg ml^{-1} acetyl-LDL and 10 μg ml^{-1} 58035; or acetyl-LDL, 58035 and 70 nM U18666A. Representative tracings of the 340:380-nm Fura-2 fluorescence ratio in an individual macrophage from each treatment group before and after addition of 1 μM thapsigargin are shown. (**b**) Plot of basal-to-peak Fura-2 fluorescence ratio after addition of thapsigargin in individual cells in each treatment group, with the mean increment denoted by the red line.

endoplasmic reticulum membranes. Signalling in the UPR is initiated by endoplasmic-reticulum-localized transmembrane protein kinases that become phosphorylated under conditions of impaired organelle function[15]. These kinases, in turn, activate downstream transcription factors that induce genes involved in restoring endoplasmic reticulum function and, when stress is severe, induce programmed cell death[15].

The downstream transcription factor CHOP (also known as GADD153) is a marker for UPR activation[31]. We found that induction of CHOP in free-cholesterol-loaded macrophages was comparable in magnitude with the induction elicited by tunicamycin or A23187, which activate the UPR by blocking *N*-linked glycosylation or endoplasmic reticulum calcium depletion, respectively (Fig. 3a). Blocking cholesterol traffic to endoplasmic reticulum membranes with low-dose U18666A blocked induction of CHOP in free-cholesterol-loaded macrophages (Fig. 3a, top, lane 5). As a control for the effects of U18666A, we demonstrated that androstenediol did not block induction of CHOP by free cholesterol (Fig. 3a, bottom). Importantly, U18666A did not block induction of CHOP by A23187 (Fig. 3a, top, lane 6), indicating that U18666A is neither a direct inhibitor of CHOP expression nor a general inhibitor of the UPR.

Induction of CHOP in the UPR is dependent on activation of the endoplasmic-reticulum-resident protein kinase, PERK, which induces the upstream transcription factor ATF-4 (ref. 32). PERK is specifically activated by impaired protein folding in the endoplasmic reticulum lumen, a common outcome of many perturbations of organelle function[33]. PERK is activated by *trans*-autophosphorylation, which is detected as a shift in the protein's mobility on immunoblots[33,34]. Most of the PERK extracted from macrophages migrated as a faster-mobility, inactive, dephosphorylated form (Fig. 3b, lane 1). Cholesterol loading resulted in a marked increase in the slower-mobility, active phosphorylated from of PERK, whereas low-dose U18666A, which blocks free cholesterol trafficking to the endoplasmic reticulum, blocked PERK activation in free-cholesterol-loaded macrophages (Fig. 3b, lanes 4 and 5). As predicted, the changes in PERK activation were reflected in the subsequent expression of its downstream effectors ATF-4 and CHOP, detected by immunoblotting nuclear extracts from the same cells (Fig. 3b, c). Note that exposure to the ACAT inhibitor 58035 alone or incubation with acetyl-LDL alone was sufficient to partially activate PERK (Fig. 3b, lanes 2 and 3). These observations suggest that endoplasmic reticulum function may be perturbed by even small increases in cellular free cholesterol.

To confirm the link between free cholesterol loading and the UPR, we examined the activity of a second independent signalling pathway active in the UPR. Similarly to PERK, IRE1 is an endoplasmic reticulum transmembrane protein kinase whose activity is controlled by *trans*-autophosphorylation[15], as reflected by a shift in mobility on immunoblots. In mammalian cells, endoplasmic reticulum stress-mediated IRE1 activation is absolutely required for expression of the active form of XBP-1, a transcription factor which functions as an effector for IRE1. Unlike CHOP, whose expression can be induced by other stress signals[35], XBP-1 is highly specific to the UPR[36,37]. Free cholesterol loading activated IRE1α (the isoform of IRE1 expressed in macrophages) and promoted XBP-1 expression (Fig. 3d, lane 4). Low-dose U18666A markedly attenuated both events (Fig. 3d, lane 5).

To examine further the importance of intracellular cholesterol trafficking in UPR activation, we compared the induction of ATF-4, CHOP and XBP-1 in *Npc1*$^{+/+}$ and *Npc1*$^{+/-}$ macrophages. As noted above, the *Npc1*$^{+/-}$ mutation blocks cholesterol trafficking to the endoplasmic reticulum[27] and blocks free-cholesterol-induced apoptosis (Fig. 1e). As shown in Fig. 3e, the expression of all three UPR proteins was markedly decreased in free-cholesterol-loaded *Npc1*$^{+/-}$, compared with *Npc1*$^{+/+}$ macrophages. As a control, we showed that induction of these three UPR proteins by A23187 was not blocked by the *Npc1*$^{+/-}$ mutation. In summary, these results establish that free cholesterol loading of macrophages activates the UPR and that manipulations which block cholesterol trafficking to endoplasmic reticulum membranes prevent this activation.

Free-cholesterol-induced macrophage death is thought to be an important event in the progression of atherosclerotic lesions. To determine if advanced atherosclerosis is associated with activation of the UPR, we studied the atherosclerotic lesions of fat-fed *Apoe*$^{-/-}$ mice. As *Apoe*$^{-/-}$ mice lack apolipoprotein E, they have high plasma cholesterol levels and thus develop advanced atherosclerosis[38]. CHOP expression was assessed by *in-situ* histohybridization and immunohistochemistry and found to be markedly elevated in proximal aortic lesions from *Apoe*$^{-/-}$ mice

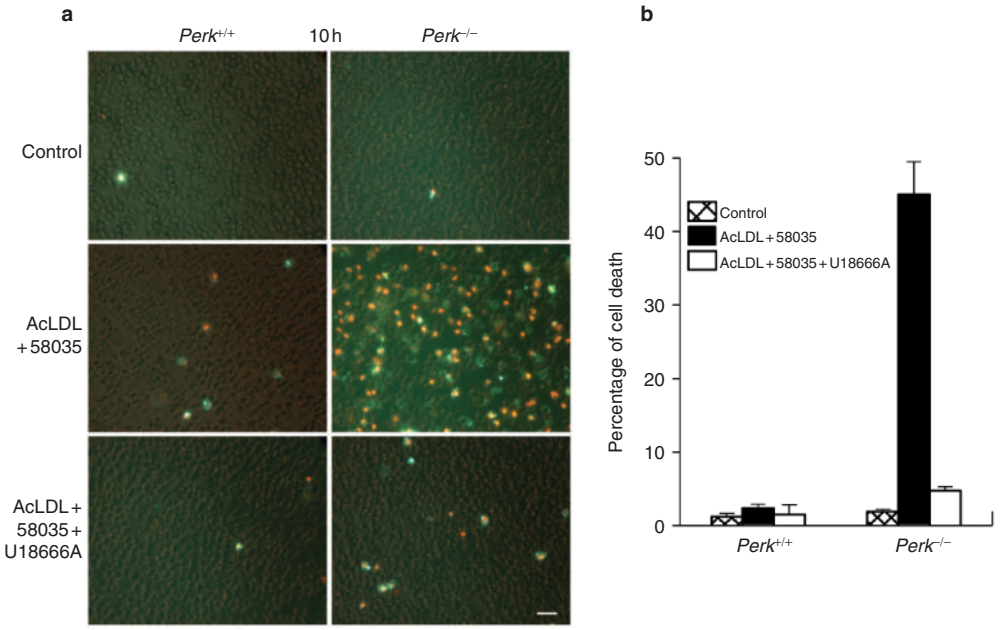

Figure 6 Disruption of the PERK enhances cholesterol-induced apoptosis. (**a**, **b**) Alexa-488–annexin V (green) and PI staining (red-orange) of macrophages from wild-type or *Perk*$^{-/-}$ mice incubated for 10 h with medium containing 100 μg ml^{-1} acetyl-LDL alone; 100 μg ml^{-1} acetyl-LDL and 10 μg ml^{-1} 58035; or acetyl-LDL, 58035 and 70 nM U18666A. Representative fluorescence images are shown in **a**. Quantitative apoptosis data from five fields of cells for each condition are shown in **b**, expressed as the percentage of total cells stained with annexin V or PI (mean ± s.e.m.; $n = 5$ fields of cells, where each field contained 200 cells). Scale bar represents 10 μm for each of the six images in **a**.

(Fig. 4a). The anti-sense signal in the histohybridization (blue) appeared to be scattered throughout the intima, being concentrated in areas that contained cells (marked by the reddish brown-stained nuclei). Staining was absent from lesions hybridized with a sense probe. *Chop* expression was also assessed by quantitative RT–PCR: we examined RNA obtained by laser-capture microdissection of macrophages from advanced atherosclerotic lesions and peritoneal macrophages from the same mice. Lesional macrophages expressed a much higher level of *Chop* mRNA (standardized with *CypA* mRNA) than peritoneal macrophages (Fig. 4b). CHOP immunostaining was widespread throughout the intima and correlated with Hoechst-3358-stained nuclei (Fig. 4c), consistent with previous localization of CHOP to the nucleus[21]. Pre-absorption of the antiserum with its cognate peptide abolished the signal (Fig 4c) and similarly, lesions stained with secondary antibody alone showed no signal (data not shown). Moreover, many of the CHOP-expressing cells in atherosclerotic lesions are in macrophage-rich (CD68-positive) and free-cholesterol-rich (filipin-positive) areas of lesions (Fig 4d). These observations demonstrate that CHOP is expressed *in vivo* under conditions of perturbed cellular cholesterol metabolism.

Endoplasmic reticulum calcium stores are depleted by free cholesterol loading

The increased free cholesterol content of endoplasmic reticulum membranes could perturb endoplasmic reticulum function at multiple levels. One possibility includes disturbance of calcium homeostasis, which depends on a calcium pump and calcium release channels embedded in the endoplasmic reticulum membrane, because depletion of endoplasmic reticulum calcium stores is a potent inducer of the UPR[39]. For example, treatment with thapsigargin, an inhibitor of the endoplasmic reticulum calcium pump, or A23187, a calcium ionophore, resulted in dysfunction of calcium-dependent endoplasmic reticulum chaperones and induced the UPR[39].

Therefore, we compared endoplasmic reticulum calcium pools in macrophages loaded with free cholesterol in the presence or absence of low-dose U18666A. Cells exposed to U18666A alone or culture media with no additives were used as further controls. After perturbing cellular cholesterol metabolism, cells were loaded with the fluorescent calcium indicator, Fura-2, switched to calcium-free medium and exposed to 1 μM thapsigargin. Thapsigargin treatment results in emptying of endoplasmic reticulum calcium stores into the cytosol, which was quantified by fluorescence microscopy, providing a measure of releasable endoplasmic reticulum calcium stores at the time of thapsigargin addition.

Representative tracings of the Fura-2 fluorescence ratio (340:380 nm) for individual macrophages in each experimental group are shown in Fig. 5a. The untreated macrophage (blue line) displayed a sharp rise in cytosolic calcium soon after addition of thapsigargin, indicating an abundance of releasable, endoplasmic-reticulum-stored calcium. Similar results were obtained using a macrophage incubated with U18666A alone (black line). In contrast, the free-cholesterol-loaded macrophage (green line) had a markedly reduced response, indicating that endoplasmic reticulum calcium stores were depleted. Macrophages loaded with free cholesterol for longer times showed no increase in cytosolic calcium after thapsigargin treatment (data not shown), indicating that endoplasmic reticulum calcium stores were severely depleted. Importantly, the macrophage loaded with free cholesterol in the presence of 70 nM U18666A (red line) showed a similar rise in cytosolic calcium as the control macrophages. Analysis of the basal-to-peak increment in fluorescence ratio of multiple individual cells in each group clearly demonstrates that free cholesterol loading is associated with a substantially smaller thapsigargin-induced rise in cytosolic calcium, an effect which is completely prevented by treatment with 70 nM U18666A (Fig. 5b). Because depletion of endoplasmic reticulum calcium stores can activate capacitive calcium entry, we

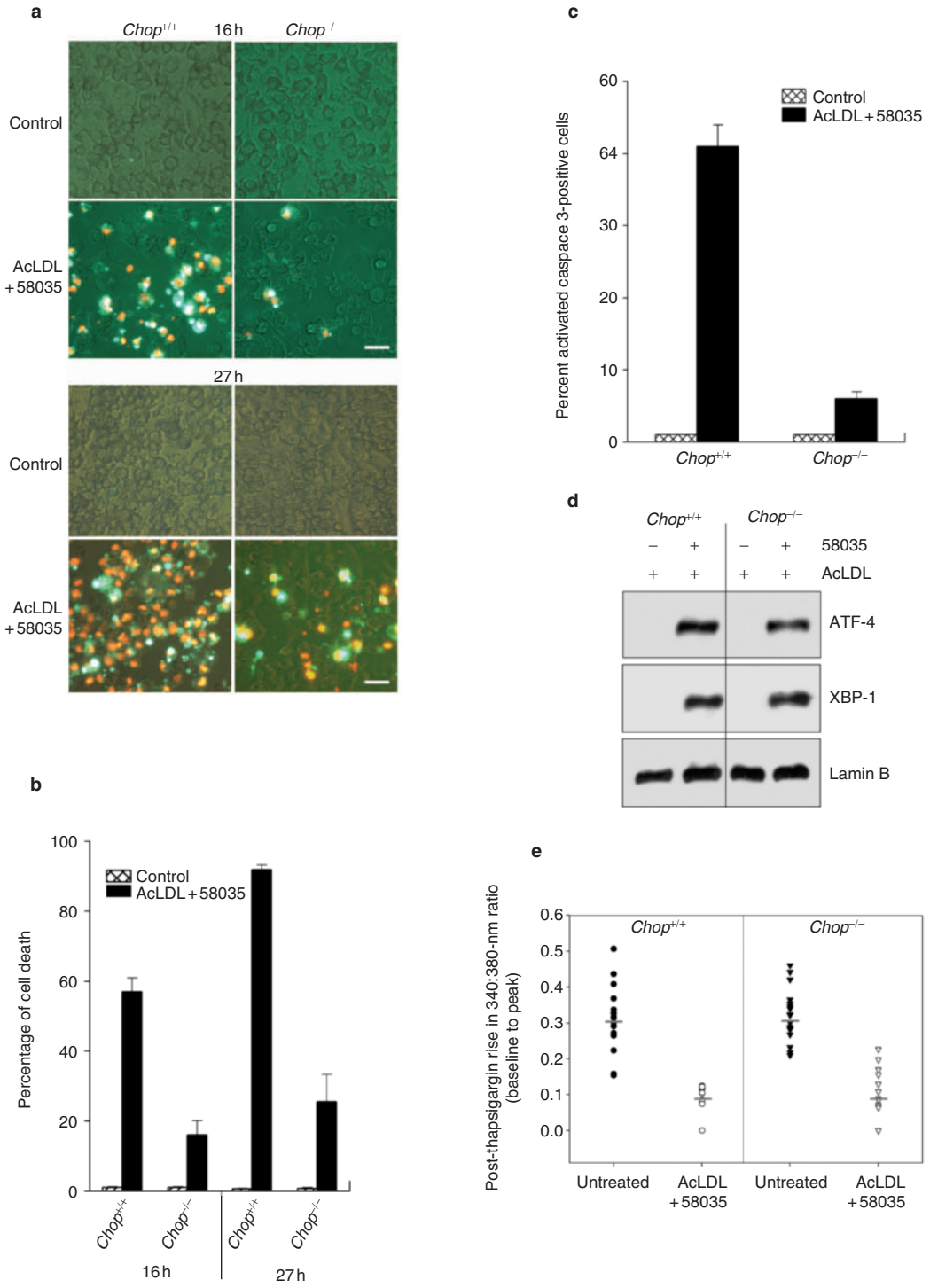

Figure 7 Disruption of CHOP attenuates free-cholesterol-induced apoptosis in macrophages. (**a**, **b**) Alexa-488–annexin V (green) and PI staining (red-orange) of macrophages from wild-type or *Chop*$^{-/-}$ mice incubated for 16 h or 27 h with medium containing 100 μg ml^{-1} acetyl-LDL alone; or acetyl-LDL and 10 μg ml^{-1} 58035. Representative fluorescence images are shown in **a**. Quantitative cell death data from five fields of cells for each condition are shown in **b**, expressed as the percentage of total cells that stained with annexin V or PI (mean ± s.e.m.; $n = 5$ fields of cells, where each field contained approximately 200 cells). Scale bars represent 10 μm in **a**. (**c**) Percentage of control and free-cholesterol-loaded *Chop*$^{+/+}$ and *Chop*$^{-/-}$ macrophages with activated caspase-3. (**d**) ATF-4, XBP-1, and lamin B immunoblots of macrophages from *Chop*$^{+/+}$ or *Chop*$^{+/+}$ mice incubated under the same conditions in Fig. 3b and d. (**e**) Plot of basal-to-peak Fura-2 fluorescence ratio after addition of thapsigargin, which is a measure of the level of endoplasmic reticulum calcium stores. Measurements were made in control and free-cholesterol-loaded macrophages from *Chop*$^{+/+}$ or *Chop*$^{+/+}$ mice, with the mean increment denoted by the horizontal line. Experimental conditions were the same as those in Fig. 4.

determined the effect of blockers of this process on free-cholesterol-induced apoptosis and CHOP induction. Although SKF96365 could not be used because of non-specific effects on cholesterol metabolism, we showed that neither 0.1 mM nickel chloride nor 10 μM cadmium succinate affected apoptosis or CHOP induction in free-cholesterol-loaded macrophages. Thus, depletion of endoplasmic reticulum calcium stores is an early event in free cholesterol loading that is dependent on intracellular cholesterol trafficking to the endoplasmic reticulum. Given that endoplasmic reticulum calcium depletion is a known inducer of the UPR, this event most probably contributes to free-cholesterol-induced UPR activation.

UPR signalling modulates free-cholesterol-induced apoptosis in macrophages

UPR signalling is important in modulating the sensitivity of cells to death induced by perturbations that cause endoplasmic reticulum stress. Cells lacking PERK are markedly hypersensitive to agents that cause endoplasmic reticulum stress[32]. In addition, animals harbouring PERK mutations undergo rapid loss of specific secretory cell populations that are exposed to physiologically high levels of endoplasmic reticulum stress[40,41]. In contrast, CHOP is an effector of cell death induced by endoplasmic reticulum stress, as *Chop*$^{-/-}$ cells are partially protected from death induced by agents and conditions that impair endoplasmic reticulum function[21,22,42]. Therefore, the signal transduction pathways downstream of PERK have protective effects that predominate, but also include a CHOP-dependent, death-promoting arm that can be selectively inactivated by deletion of CHOP.

If endoplasmic reticulum dysfunction is important in the death of free-cholesterol-loaded macrophages, deletion of PERK should increase cell death, whereas deletion of CHOP should protect against death. Therefore, we compared the response to free cholesterol loading of macrophages from wild-type, *Chop*$^{-/-}$ and *Perk*$^{-/-}$ mice. Cell death, as measured by annexin V and propidium iodide (PI) staining, was markedly increased in free-cholesterol-loaded *Perk*$^{-/-}$ macrophages, compared with wild-type macrophages (Fig. 6a, b). Importantly, a low dose of U18666A provided significant protection to *Perk*$^{-/-}$ cells, suggesting that free cholesterol trafficking to the endoplasmic reticulum is important for the death of *Perk*$^{-/-}$ cells (Fig. 6a, b).

In contrast, the majority of *Chop*$^{-/-}$ macrophages were protected from cell death induced by free cholesterol loading. Furthermore, this protection was noted at both early (16 h) and late times (27 h), relative to the wild-type cells (Fig. 7a, b). The percentage of macrophages containing activated caspase-3, which is critical for free-cholesterol-induced apoptosis[10], was also markedly decreased in the *Chop*$^{-/-}$ macrophages (Fig. 7c). Neither the *Perk* nor the *Chop* mutations significantly affected the mass of lipoprotein-free cholesterol accumulated by the macrophages (data not shown). These data establish a functional role for the UPR in free-cholesterol-induced apoptosis in macrophages. Moreover, consistent with the notion that the *Chop*$^{-/-}$ mutation blocks free-cholesterol-induced macrophage death through a distal UPR pathway, and not by inhibiting upstream events, induction of XBP-1 and ATF-4, as well as depletion of endoplasmic reticulum calcium stores, were similar in free-cholesterol-loaded *Chop*$^{+/+}$ and *Chop*$^{-/-}$ macrophages (Fig. 7d, e).

DISCUSSION

Cells possess multiple mechanisms to prevent the accumulation of excess free cholesterol, including activation of ACAT-mediated cholesterol esterification and cellular cholesterol efflux[8]. When one or more of these mechanisms fail, as seems to occur in macrophages in advanced atherosclerotic lesions, cell death ensues. The intracellular accumulation of large amounts of cholesteryl ester, as occurs in the macrophage foam cells of early atherosclerotic lesions, does not induce cell death. The fact that cholesteryl esters are stored in relatively inert intracellular lipid vesicles, whereas free cholesterol is integrated into the lipid bilayers of cellular membranes, has been proposed as a possible clue to the toxic effects of the latter. The purpose of this study was to provide insight into the perturbations affected by free cholesterol loading of macrophages.

We reasoned that elucidating the site of free cholesterol accumulation might provide a clue to the mechanism of free-cholesterol-induced toxicity. Although the direct measurement of free cholesterol mass in biological membranes is difficult, plasma membrane free cholesterol content can be estimated by both the cholesterol oxidase method[43] and by availability to cyclodextrin-mediated efflux[44]. In addition, endoplasmic reticulum cholesterol can be assessed by esterification through ACAT[45]. Using these methods, we showed that both low-dose U18666A and the *Npc1*$^{+/-}$ mutation, which inhibit free cholesterol trafficking to the endoplasmic reticulum but not to the plasma membrane, block macrophage apoptosis. Moreover, directly loading the plasma membrane with free cholesterol did not induce apoptosis. Free cholesterol loading of mitochondria is also unlikely to contribute to macrophage death, because incubation of mitochondria with excess cholesterol *in vitro* actually stabilizes mitochondrial function (ref. 46; P.M.Y. and I.T., unpublished observations). In contrast to the plasma membrane, the endoplasmic reticulum membrane is fluid and low in cholesterol[14], and is thus predicted to be particularly sensitive to the toxic effects of free cholesterol enrichment. Indeed, we find that an endoplasmic-reticulum-based stress pathway is induced by free cholesterol loading. Together, these findings suggest that the endoplasmic reticulum is a major source of free-cholesterol-induced apoptosis.

We wondered how free cholesterol trafficking to endoplasmic reticulum membranes might result in endoplasmic reticulum stress. Integral membrane endoplasmic reticulum proteins that are essential to proper organelle function may be perturbed by increasing the free cholesterol:phospholipid ratio of the normally fluid endoplasmic reticulum membrane. In this report, we have shown that a critical endoplasmic reticulum membrane-protein-dependent function, namely, maintenance of endoplasmic reticulum calcium homeostasis is perturbed early in the course of free cholesterol loading. The fact that this effect required cholesterol trafficking to the endoplasmic reticulum membrane and that depletion of endoplasmic reticulum calcium stores by other agents induces the UPR suggests that this event is at least part of the mechanism linking free cholesterol loading to UPR induction. It is also possible that free cholesterol loading of the endoplasmic reticulum membrane perturbs other endoplasmic reticulum membrane-dependent activities, either as a primary event or secondary to the early depletion of endoplasmic reticulum calcium stores. Interestingly, modest levels of free cholesterol loading are sufficient to activate the PERK kinase in macrophages (Fig. 3b), suggesting that the endoplasmic reticulum in these cells may normally function close to its threshold for free cholesterol tolerance.

An important finding in this report is that UPR signalling has a profound effect on free-cholesterol-induced macrophage apoptosis. The fact that *Perk*$^{-/-}$ macrophages are markedly hypersensitive to free cholesterol loading indicates that the ability to resist endoplasmic reticulum stress can be limiting for the survival of free-cholesterol-loaded macrophages. Alternatively, the finding that the majority of *Chop*$^{-/-}$ macrophages are resistant to free-cholesterol-induced cell death and caspase-3 activation argues that a pro-apoptotic pathway activated specifically by the CHOP arm of the UPR is important for promoting apoptosis under these circumstances. Possible mechanisms include

CHOP-induced decreases in Bcl-2 and glutathione and increases in reactive oxygen species[42]. Non-CHOP pathways of apoptosis may also be involved, as approximately 30% of free-cholesterol-induced macrophage death occurs in the presence of the *Chop*$^{-/-}$ mutation. Nonetheless, the fact that CHOP is expressed in macrophage and free-cholesterol-rich areas of atherosclerotic lesions, that advanced lesional macrophages accumulate free cholesterol and that macrophage death is associated with plaque disruption suggest that endoplasmic reticulum stress in lesional macrophages may be an important cellular process in the progression of atherosclerosis.

Note added in proof: in a recent study, (Feng, B., et al. *Niemann-Pick C heterozygosity confers resistance to lesional necrosis and macrophage apoptosis in murine atherosclerosis.* Proc. Natl Acad. Sci. USA *(in the press)), we demonstrate that macrophage apoptosis and lesional necrosis are substantially decreased in the atherosclerotic lesions of* Apoe$^{-/-}$ *mice on the* Npc1$^{+/-}$ *background versus the* Npc1$^{+/+}$ *background, thus providing* in vivo *evidence that trafficking of cholesterol to the endoplasmic reticulum is important in lesional macrophage apoptosis and plaque morphology.* □

METHODS

Materials. Falcon tissue culture plastic was purchased from Fisher Scientific (Springfield, NJ). Tissue culture media and other tissue culture reagents were obtained from Invitrogen (Carlsbad, CA). Foetal bovine serum (FBS) was obtained from Hyclone Laboratories (Logan, UT) and was heat-inactivated for 1 h at 65 °C (HI-FBS). Compound 58035 (3-[decyldimethylsilyl]-*N*-[2-(4-methylphenyl)-1-phenylethyl]propanamide[47], an inhibitor of ACAT, was generously provided by J. Heider, formerly of Sandoz (East Hanover, NJ); a 10 mg ml^{-1} stock solution was prepared in dimethyl sulphoxide (DMSO), and the final DMSO concentration in both treated and control cells was 0.05%. Cholesterol (>99% pure) was obtained from Nu-chek Prep. (Elysian, MN). U18666A (3-β [2-diethylaminoethoxy]androst-5-en-17-one hydrochloride) was from Biomol (Plymouth Meeting, PA). LDL (*d,* 1.020–1.063 g ml^{-1}) from fresh human plasma was isolated by preparative ultracentrifugation. Acetyl-LDL was prepared by reaction with acetic anhydride[48]. All other chemicals and reagents, including androstenediol, *Streptomyces* (Sigma, St Louis, MO) cholesterol oxidase, methyl-β-cyclodextrin, concanavalin A, A32187, thapsigargin, tunicamycin and the anti-β-actin monoclonal antibody were from Sigma, and all organic solvents were from Fisher Scientific. Methyl-β-CD was saturated with cholesterol as previously described[29]. Anti-GADD153 (CHOP) was from Santa Cruz Biotechnology (Santa Cruz, CA). Antibodies against XBP-1, ATF-4, PERK and IRE1α were made as described[34,35,37]. Horseradish peroxidase (HRP)-conjugated goat anti-rabbit IgG and goat anti-mouse IgG were from Bio-Rad (Hercules, CA) and rabbit anti-lamin B polyclonal antiserum was a generous gift from E. Marcantonio (Department of Pathology, Columbia University, NY).

Mice. *Apoe*$^{-/-}$ mice on the C57BL/6 background were fed after weaning a high-cholesterol diet containing 21% anhydrous milk fat and 0.15% cholesterol ("Western-type" diet; Harlan-Teklad, Indianapolis, IN) for the indicated times. *Chop*$^{-/-}$ mice on the FVB/N background and *Perk*$^{-/-}$ mice on the Swiss-Webster background were created as previously described[21,32]. For experiments involving these mice, control macrophages were obtained from wild-type siblings.

Free cholesterol loading and cell death assays of mouse peritoneal macrophages. Peritoneal macrophages from adult female C57BL/6 mice and all mutant mice used in this study were harvested three days after intraperitoneal injection of 40 μg concanavalin A in 0.5 ml of PBS. Cells were incubated in DMEM supplemented with 10% FBS and 20% L-cell-conditioned medium. The medium was replaced every 24 h until macrophages were confluent. On the day of the experiment, cells were washed three times with warmed PBS and incubated as indicated in the figure legends. Most importantly, free cholesterol loading of wild-type and mutant macrophages was effected by incubating the cells with 100 μg ml^{-1} acetyl-LDL in the presence of 10 μg ml^{-1} 58035, which inhibits ACAT-mediated cholesterol esterification[10]. At the end of the incubation period, macrophages were assayed for early-to-mid-stage apoptosis (that is, externalization of phosphatidylserine) by staining with Alexa-488-labelled annexin V and for late-stage apoptosis (that is, increased membrane permeability) by staining with PI, as previously described[10]. Cells were viewed immediately with an Olympus IX-70 inverted fluorescence microscope, and 3–6 representative fields (approximately 1,000 cells) for each condition were counted for the number of annexin-positive, PI-positive cells, and total cells. In other experiments, cell or nuclear preparations were subjected to immunoblot analysis, as described below. Activated caspase-3 in macrophages was detected by immunofluorescence microscopy using an antibody that specifically recognizes the active form (Apo-Active 3 kit; Cell Technology, Minneapolis, MN).

Whole-cell cholesterol esterification assay. Macrophages were incubated for 5 h with DMEM, 0.2% BSA containing 50 μg ml^{-1} ^{3}H-cholesterol-labelled acetyl-LDL alone or containing the indicated compounds. Cellular lipids were extracted twice with 0.5 ml of hexane:isopropanol (3:2, v:v), and the cellular content of ^{3}H-cholesteryl ester was determined using thin-layer chromatography[49]. The lipid-extracted cell monolayer was dissolved in 1 ml 1 N NaOH and assayed for protein content using the Lowry method[50].

Cholesterol oxidase assay. Macrophages were fixed with 1% glutaraldehyde for 10 min and then incubated for 30 min at 37 °C with 2 U ml^{-1} *Streptomyces* cholesterol oxidase. Cellular lipids were extracted twice with 0.5 ml of hexane:isopropanol (3:2). Cholesterol and cholestenone mass in these extracts were determined by gas–liquid chromatography using β-sitosterol as an internal standard. The lipid-extracted cell monolayer was dissolved in 1 ml 1 N NaOH and assayed for protein content using the Lowry method[50].

Immunoblot analysis. Immunoprecipitation and immunoblotting of IRE1α and PERK were conducted as previously described[34]. Immunoblotting of XBP-1, ATF-4 and CHOP were performed as previously described[35,37] with minor modifications. Briefly, cells were lysed in RIPA buffer to prepare whole-cell lysates or to prepare nuclei by centrifugation. The whole-cell lysates or nuclei were resuspended in 2× SDS–polyacrylamide gel electrophoresis (PAGE) loading buffer and incubated at 95 °C for 10 min. Whole-cell (100 μg) or nuclear (20 μg) lysates were electrophoresed on 4–20% gradient SDS–PAGE gels and electrotransferred to 0.22-μm nitrocellulose membranes using a Bio-Rad mini-transfer tank. After incubation with primary antibodies, the protein bands were detected with HRP-conjugated secondary antibodies (Bio-Rad) and by ECL (Amersham Pharmacia Biotech, Piscataway, NJ). Membranes were reprobed with an anti-β-actin monoclonal antibody or an anti-lamin B serum to control for differences in loading.

Assay of endoplasmic reticulum calcium pools. Untreated or cholesterol-loaded macrophages grown on 25-mm coverslips in microscopy dishes were loaded with 4 μM Fura-2 a.m. (Molecular Probes, Eugene, OR) and 0.08% Pluronic F-127 in Hank's buffered saline solution (HBSS) at room temperature for 30 min. Monolayers were then washed twice with HBSS, incubated in HBSS for an additional 30 min and then mounted on the stage of an inverted Nikon diaphot microscope equipped with a 40× objective. Sulphinpyrazone (250 μM) was included in all solutions to prevent excretion of the Fura-2 by macrophages. Fluorescence images (510-nm emission after alternate 340- and 380-nm excitation) were collected through a charge-coupled device camera (Photon Technology International, Lawrenceville, NJ) and the 340:380 ratio of individual cells in these images was calculated.

***In-situ* hybridization.** The 470-bp *BamH*I-*Nhe*I fragment of CHOP was subcloned into the *BamH*I and *Xba*I sites of the pCRII-TOPO vector (Invitrogen). The resulting plasmid was transcribed *in vitro* using the DIG-RNA Labelling kit (SP6–T7; Roche Molecular Biochemicals, Basel, Switzerland) to generate sense and anti-sense Dig–ribo probes. Proximal aortae from *Apoe*$^{-/-}$ mice fed the Western-type diet for 13 weeks were fixed in 4% paraformaldehyde in PBS at 4 °C overnight and then submerged in 30% (w/v) sucrose in PBS for 48 h at 4 °C. The tissue was then embedded in optimal cutting temperature (OCT) embedding medium (VWR Scientific, Bridgeport, NJ), cut into 10-μm sections and mounted on Superfrost-plus slides (Fisher Scientific). Sections were then fixed in 4% paraformaldehyde for 10 min, washed with PBS and treated for 10 min each with 10 μg ml^{-1} proteinase K in 50 mM Tris-HCl, 5 mM EDTA at pH 8.0 and then 0.25% acetic anhydride in 0.1 M triethanolamine at pH 8.0.

Slides were dehydrated by sequential 5-min incubations with 70%, 85%, 95% and 100% ethanol, followed by incubation in xylene. Sections were then incubated for 2 h at 42 °C with 200 µl of prehybridization buffer, which contained 50% formamide, 4× SSC, 5× Denhardt's solution, 500 µg ml^{-1} denatured salmon sperm DNA and 250 µg ml^{-1} yeast RNA. For hybridization, sections were incubated for 24 h at 42 °C with 80 µl of the above buffer containing 1 µg ml^{-1} sense or anti-sense DIG-labelled RNA probe. Next, sections were incubated sequentially as follows: 30 min at 42 °C with 50% formamide and 1× SSC; 15 min at 37 °C with 0.5× SSC; 15 min at 37 °C with 3.5× SSC containing 20 µg ml^{-1} RNase A; 15 min at room temperature with 3.5× SSC; and 60 min at 60 °C with 0.1× SSC. For signal detection, sections were incubated for 2 h with anti-DIG alkaline phosphatase-conjugated antibody (1:200), washed with PBS and then developed with alkaline phosphatase substrate (Roche Molecular Biochemicals) for 16 h. Sections were then dehydrated, rehydrated and counterstained with 3% neutral red for 5 min.

Laser capture microdissection (LCM) and RNA extraction. Aortic roots with atherosclerotic lesions were removed from *Apoe*$^{-/-}$ mice that had been fed the Western-type diet for 13 weeks. The roots were embedded in OCT compound (VWR Scientific) and frozen immediately on dry ice. Cryostat sections (6-µm thickness) were mounted on positively charged slides (Colour Frost Plus; Fisher Scientific). Lesional macrophage RNA was procured by LCM using a PixCell II LCM System (Arcturus, Mountain View, CA), as previously described[51]. Briefly, the macrophages of dehydrated sections were stained with an anti-CD68 antibody (Serotec, Raleigh, NC) and the positively stained areas were selected and affixed to thermoplastic film mounted on optically transparent LCM caps (Arcturus). Total RNA was isolated from selected cells using a Picopure RNA Isolation Kit (Arcturus) in accordance with the manufacturer's instructions before treatment with DNase I (Ambion, Austin, TX). RNA concentrations were determined using a RiboGreen RNA Quantitation Kit (Molecular Probes).

Quantitative RT–PCR. Total RNA from resident peritoneal macrophages or from lesional macrophages, obtained by laser-capture microdissection, was reverse-transcribed into cDNA using oligo-dT and Superscript II (Invitrogen). Quantitative PCR for *Chop* and *cyclophilin A* (*CypA*) was conducted using the Taqman PCR reagent (ABI) and the ABI PRISM 7700 sequence detection system, as previously described[51]. For *Chop*, the forward and reverse primers were CCACCACACCTGAAAGCAGAA and AGGTGAAAGGCAGGGACTCA, respectively, and the probe was 6FAM-CTGGTCCACGTGCAGTCATGG-TAMRA. For *CypA*, the forward and reverse primers were GGCCGATGAC-GAGCCC and TGTCTTTGGAACTTTGTCTGCAA, respectively, and the probe was TGTCTTTGGAACTTTGTCTGCAA. The PCR conditions for *Chop* cDNA detection were 95 °C for 1 min, 58 °C for 30 s and 72 °C for 30 s, for 40 cycles. For *CypA*, the conditions were 95 °C for 1 min and 60 °C for 10 s, for 40 cycles.

Immunofluorescence microscopic detection of CHOP and CD68 in atherosclerotic lesions. Mice were anaesthetized, blood was withdrawn by cardiac puncture, and the heart was perfused with PBS and then 4% paraformaldehyde. The heart and proximal aorta were harvested and perfused *ex vivo* with 4% paraformaldehyde and then stored in the same fixative for 16 h at 4 °C. Specimens were then transferred to 30% sucrose in PBS for 48 h at 4 °C. In preparation for sectioning, the hearts were embedded in OCT compound and stored at −70 °C. Sections (10 µm) of the proximal aorta were prepared at −20 °C on a Microm (Walldorf, Baden, Germany) microtome cryostat HM 505E, placed on poly-L-lysine-coated glass slides and briefly air dried. Sections were washed in PBS and permeabilized in PBS containing 0.2% Triton X-100 for 10 min, washed in PBS containing 0.05% Tween-20 for 10 min and then rinsed repeatedly with PBS alone at room temperature. Blocking was accomplished by incubation with 5% normal goat serum in PBS for 16 h at 4 °C before washing in PBS containing 0.05% Tween-20 for 10 min and rinsing repeatedly with PBS at room temperature. For interaction with primary antibodies, the sections were incubated with 2.5% goat serum containing 1 µg ml^{-1} rabbit polyclonal anti-CHOP carboxy-terminal peptide IgG (R-20 from Santa Cruz Biotechnology) or 1:500 rat monoclonal anti-CD68 supernatant (FA11 from Serotec) for 1 h at room temperature. In control experiments, the anti-CHOP IgG was pre-absorbed with a fivefold mass excess of the C-terminal peptide before addition to slides. After the sections were washed in PBS containing Tween-20 and then PBS, the bound primary antibody was visualized with 7.5 µg ml^{-1} Cy3-conjugated goat anti-rabbit IgG or 3 µg ml^{-1} Cy3-conjugated goat anti-rat IgG (Jackson ImmunoResearch Laboratories, West Grove, PA). Sections were then washed in PBS. For the CHOP experiment, DNA was stained with the karyophilic dye Hoechst 33258 (140 ng ml^{-1}) for 1 min at room temperature. After extensive washing in PBS, the slides were mounted with a coverslip and viewed with an Olympus IX 70 inverted fluorescence microscope equipped with a CoolSNAP CCD camera.

Filipin staining of aortic sections. Frozen sections of proximal aorta were washed in PBS and then fixed with fresh 3% formaldehyde for 1 h at room temperature. The fixed sections were washed with PBS for 10 min to quench the formaldehyde and then incubated with 0.05 mg ml^{-1} filipin solution for 2 h at room temperature. After washing in PBS, sections were viewed by fluorescence microscopy using an Olympus IX 70 inverted microscope equipped with a UV filter set (340–380-nm excitation, 400-nm dichroic and 430-nm long-pass filters).

Statistics. Results are given as means ± s.e.m.; $n = 3$ unless otherwise stated.

ACKNOWLEDGEMENTS

This work was supported by National Institutes of Health (NIH) grants HL54591, HL57560 and HL56984 to I.T, DK47119 and ES08681 to D.R. and HL61814 to E.A.F. We gratefully acknowledge R. Soccio and F. Wang for assistance with the CHOP Taqman and *in-situ* hybridization assays, respectively. We also thank Y. Zhang for technical assistance and R. Jungreis for help with the *Perk*$^{-/-}$ and *Chop*$^{-/-}$ mice.

COMPETING FINANCIAL INTERESTS

The authors declare that they have no competing financial interests.

Received 12 March 2003; accepted 10 July 2003;
Published online at http://www.nature.com/naturecellbiology

1. Shio, H., Haley, N. J. & Fowler, S. Characterization of lipid-laden aortic cells from cholesterol-fed rabbits. III. Intracellular localization of cholesterol and cholesteryl ester. *Lab. Invest.* **41,** 160–167 (1979).
2. Rapp, J. H., Connor, W. E., Lin, D. S., Inahara, T. & Porter, J. M. Lipids of human atherosclerotic plaques and xanthomas: clues to the mechanism of plaque progression. *J. Lipid Res.* **24,** 1329–1335 (1983).
3. Small, D. M., Bond, M. G., Waugh, D., Prack, M. & Sawyer, J. K. Physicochemical and histological changes in the arterial wall of non-human primates during progression and regression of atherosclerosis. *J. Clin. Invest.* **73,** 1590–1605 (1984).
4. Kruth, H. S. & Fry, D. L. Histochemical detection and differentiation of free and esterified cholesterol in swine atherosclerosis using filipin. *Exp. Mol. Pathol.* **40,** 288–294 (1984).
5. Libby, P. & Clinton, S. K. The role of macrophages in atherogenesis. *Curr. Opin. Lipidol.* **4,** 355–363 (1993).
6. Ball, R. Y. *et al.* Evidence that the death of macrophage foam cells contributes to the lipid core of atheroma. *Atherosclerosis* **114,** 45–54 (1995).
7. Fazio, S. *et al.* Increased atherosclerosis in LDL receptor-null mice lacking ACAT1 in macrophages. *J. Clin. Invest.* **107,** 163–171 (2001).
8. Tabas, I. Consequences of cellular cholesterol accumulation: basic concepts and physiological implications. *J. Clin. Invest.* **110,** 905–911 (2002).
9. Kellner-Weibel, G. *et al.* Effects of intracellular free cholesterol accumulation on macrophage viability: a model for foam cell death. *Arterioscler. Thromb. Vasc. Biol.* **18,** 423–431 (1998).
10. Yao, P. M. & Tabas, I. Free cholesterol loading of macrophages induces apoptosis involving the fas pathway. *J. Biol. Chem.* **275,** 23807–23813 (2000).
11. Yao, P. M. & Tabas, I. Free cholesterol loading of macrophages is associated with widespread mitochondrial dysfunction and activation of the mitochondrial apoptosis pathway. *J. Biol. Chem.* **276,** 42468–42476 (2001).
12. Kellner-Weibel, G., Geng, Y. J. & Rothblat, G. H. Cytotoxic cholesterol is generated by the hydrolysis of cytoplasmic cholesteryl ester and transported to the plasma membrane. *Atherosclerosis* **146,** 309–319 (1999).
13. Yeagle, P. L. Modulation of membrane function by cholesterol. *Biochimie* **73,** 1303–1310 (1991).
14. Bretscher, M. S. & Munro, S. Cholesterol and the Golgi apparatus. *Science* **261,** 1280–1281 (1993).
15. Patil, C. & Walter, P. Intracellular signaling from the endoplasmic reticulum to the nucleus: the unfolded protein response in yeast and mammals. *Curr. Opin. Cell Biol.* **13,** 349–355 (2001).
16. Travers, K. J. *et al.* Functional and genomic analyses reveal an essential coordination between the unfolded protein response and ER-associated degradation. *Cell* **101,** 249–258 (2000).
17. Zhang, D. *et al.* Macrophages deficient in CTP:Phosphocholine cytidylyltransferase-α are viable under normal culture conditions but are highly susceptible to free cholesterol-induced death. Molecular genetic evidence that the induction of phosphatidylcholine biosynthesis in free cholesterol-loaded macrophages is an adaptive response. *J. Biol. Chem.* **275,** 35368–35376 (2000).

18. Nakagawa, T. *et al.* Caspase-12 mediates endoplasmic-reticulum-specific apoptosis and cytotoxicity by amyloid-β. *Nature* **403,** 98–103 (2000).
19. Urano, F. *et al.* Coupling of stress in the ER to activation of JNK protein kinases by transmembrane protein kinase IRE1. *Science* **287,** 664–666 (2000).
20. Nishitoh, H. *et al.* ASK1 is essential for endoplasmic reticulum stress-induced neuronal cell death triggered by expanded polyglutamine repeats. *Genes Dev.* **16,** 1345–1355 (2002).
21. Zinszner, H. *et al.* CHOP is implicated in programmed cell death in response to impaired function of the endoplasmic reticulum. *Genes Dev.* **12,** 982–995 (1998).
22. Oyadomari, S. *et al.* Targeted disruption of the *Chop* gene delays endoplasmic reticulum stress-mediated diabetes. *J. Clin. Invest.* **109,** 525–532 (2002).
23. Underwood, K. W., Andemariam, B., McWilliams, G. L. & Liscum, L. Quantitative analysis of hydrophobic amine inhibition of intracellular cholesterol transport. *J. Lipid Res.* **37,** 1556–1568 (1996).
24. Shiratori, Y., Okwu, A. K. & Tabas, I. Free cholesterol loading of macrophages stimulates phosphatidylcholine biosynthesis and up-regulation of CTP:phosphocholine cytidylyltransferase. *J. Biol. Chem.* **269,** 11337–11348 (1994).
25. Aikawa, K., Furuchi, T., Fujimoto,Y., Arai, H. & Inoue, K. Structure-specific inhibition of lysosomal cholesterol transport in macrophages by various steroids. *Biochim. Biophys. Acta* **1213,** 127–134 (1994).
26. Liscum, L. & Klansek, J. J. Niemann-Pick disease type C. *Curr. Opin. Lipidol.* **9,** 131–135 (1998).
27. Feng, B. & Tabas, I. ABCA1-mediated cholesterol efflux is defective in free cholesterol-loaded macrophages. Mechanism involves enhanced ABCA1 degradation in a process requiring full NPC1 activity. *J. Biol. Chem.* **277,** 43271–43280 (2002).
28. Yancey, P. G. *et al.* Cellular cholesterol efflux mediated by cyclodextrins. Demonstration of kinetic pools and mechanism of efflux. *J. Biol. Chem.* **271,** 16026–16034 (1996).
29. Christian, A. E., Haynes, M. P., Phillips, M. C. & Rothblat, G. H. Use of cyclodextrins for manipulating cellular cholesterol content. *J. Lipid Res.* **38,** 2264–2272 (1997).
30. Khan, N. *et al.* Plasma membrane cholesterol: A possible barrier to intracellular oxygen in normal and mutant CHO cells defective in cholesterol metabolism. *Biochemistry* **42,** 23–29 (2003).
31. Wang, X. Z. & Ron, D. Stress-induced phosphorylation and activation of the transcription factor CHOP (GADD153) by p38 MAP Kinase. *Science* **272,** 1347–1349 (1996).
32. Harding, H. P., Zhang, Y., Bertolotti, A., Zeng, H. & Ron, D. Perk is essential for translational regulation and cell survival during the unfolded protein response. *Mol. Cell* **5,** 897–904 (2000).
33. Bertolotti, A., Zhang, Y., Hendershot, L. M., Harding, H. P. & Ron, D. Dynamic interaction of BiP and ER stress transducers in the unfolded-protein response. *Nature Cell Biol.* **2,** 326–332 (2000).
34. Harding, H. P., Zhang, Y. & Ron, D. Protein translation and folding are coupled by an endoplasmic-reticulum-resident kinase. *Nature* **397,** 271–274 (1999).
35. Harding, H. P. *et al.* Regulated translation initiation controls stress-induced gene expression in mammalian cells. *Mol. Cell* **6,** 1099–1108 (2000).
36. Yoshida, H., Matsui, T., Yamamoto, A., Okada, T. & Mori, K. *XBP1* mRNA is induced by ATF6 and spliced by IRE1 in response to ER stress to produce a highly active transcription factor. *Cell* **107,** 881–891 (2001).
37. Calfon, M. *et al.* IRE1 couples endoplasmic reticulum load to secretory capacity by processing the *XBP-1* mRNA. *Nature* **415,** 92–96 (2002).
38. Plump, A. S. *et al.* Severe hypercholesterolemia and atherosclerosis in apolipoprotein E-deficient mice created by homologous recombination in ES cells. *Cell* **71,** 343–353 (1992).
39. Treiman, M. Regulation of the endoplasmic reticulum calcium storage during the unfolded protein response — significance in tissue ischemia? *Trends Cardiovasc. Med.* **12,** 57–62 (2002).
40. Harding, H. P. *et al.* Diabetes mellitus and exocrine pancreatic dysfunction in *Perk*$^{-/-}$ mice reveals a role for translational control in secretory cell survival. *Mol. Cell* **7,** 1153–1163 (2001).
41. Zhang, P. *et al.* The PERK eukaryotic initiation factor 2α kinase is required for the development of the skeletal system, postnatal growth, and the function and viability of the pancreas. *Mol. Cell Biol.* **22,** 3864–3874 (2002).
42. McCullough, K. D., Martindale, J. L., Klotz, L. O., Aw, T. Y. & Holbrook, N. J. Gadd153 sensitizes cells to endoplasmic reticulum stress by down-regulating Bcl2 and perturbing the cellular redox state. *Mol. Cell Biol.* **21,** 1249–1259 (2001).
43. Lange, Y. Tracking cell cholesterol with cholesterol oxidase. *J. Lipid Res.* **33,** 315–321 (1992).
44. Lange, Y., Ye, J., Rigney, M. & Steck, T. L. Cholesterol movement in Niemann-Pick Type C cells and in cells treated with amphiphiles. *J. Biol. Chem.* **275,** 17468–17475 (2000).
45. Lange, Y. & Steck, T. L. Quantitation of the pool of cholesterol associated with acyl-CoA:cholesterol acyltransferase in human fibroblasts. *J. Biol. Chem.* **272,** 13103–13108 (1997).
46. Graham, J. M. & Green, C. The properties of mitochondria enriched *in vitro* with cholesterol. *Eur. J. Biochem.* **12,** 58–66 (1970).
47. Ross, A. C., Go, K. J., Heider, J. G. & Rothblat, G. H. Selective inhibition of acyl coenzyme A:cholesterol acyltransferase by compound 58–035. *J. Biol. Chem.* **259,** 815–819 (1984).
48. Basu, S. K., Goldstein, J. L., Anderson, R. G. W. & Brown, M. S. Degradation of cationized low density lipoprotein and regulation of cholesterol metabolism in homozygous familial hypercholesterolemia fibroblasts. *Proc. Natl Acad. Sci. USA* **73,** 3178–3182 (1976).
49. Tabas, I., Boykow, G. & Tall, A. Rabbit liver microsomal ACAT: Smooth ER enzyme associated with a lipid ACAT inhibitor. *Arteriosclerosis* **8,** 559A (1988).
50. Lowry, O. H., Rosenbrough, N. J., Farr, A. L. & Randall, R. J. Protein measurement with the folin phenol reagent. *J. Biol. Chem.* **193,** 265–275 (1951).
51. Trogan, E. *et al.* Laser capture microdissection analysis of gene expression in macrophages from atherosclerotic lesions of apolipoprotein E-deficient mice. *Proc. Natl Acad. Sci. USA* **99,** 2234–2239 (2002).